

Adaptive Transmitter Optimization in Multiuser Multiantenna Systems: Theoretical Limits, Effect of Delays, and Performance Enhancements

Dragan Samardzija

Wireless Research Laboratory, Bell Labs, Lucent Technologies, 791 Holmdel-Keyport Road, Holmdel, NJ 07733, USA
Email: dragan@bell-labs.com

Narayan Mandayam

Wireless Information Network Laboratory (WINLAB), Rutgers University, 73 Brett Road, Piscataway, NJ 08854-8060, USA
Email: narayan@winlab.rutgers.edu

Dmitry Chizhik

Wireless Research Laboratory, Bell Labs, Lucent Technologies, 791 Holmdel-Keyport Road, Holmdel, NJ 07733, USA
Email: chizhik@bell-labs.com

Received 6 March 2005; Revised 21 April 2005

The advances in programmable and reconfigurable radios have rendered feasible transmitter optimization schemes that can greatly improve the performance of multiple-antenna multiuser systems. Reconfigurable radio platforms are particularly suitable for implementation of transmitter optimization at the base station. We consider the downlink of a wireless system with multiple transmit antennas at the base station and a number of mobile terminals (i.e., users) each with a single receive antenna. Under an average transmit power constraint, we consider the maximum achievable sum data rates in the case of (1) zero-forcing (ZF) spatial prefilter, (2) modified zero-forcing (MZF) spatial prefilter, and (3) triangularization spatial prefilter coupled with dirty-paper coding (DPC) transmission scheme. We show that the triangularization with DPC approaches the closed-loop MIMO rates (upper bound) for higher SNRs. Further, the MZF solution performs very well for lower SNRs, while for higher SNRs, the rates for the ZF solution converge to the MZF rates. An important impediment that degrades the performance of such transmitter optimization schemes is the delay in channel state information (CSI). We characterize the fundamental limits of performance in the presence of delayed CSI and then propose performance enhancements using a linear MMSE predictor of the CSI that can be used in conjunction with transmitter optimization in multiple-antenna multiuser systems.

Keywords and phrases: transmitter beamforming, dirty-paper coding, correlated channels, channel state information, MMSE prediction.

1. INTRODUCTION

For a wide range of emerging wireless data services, the application of multiple antennas appears to be one of the most promising solutions leading to even higher data rates and/or the ability to support greater number of users. Multiple-transmit multiple-receive antenna systems represent an implementation of the MIMO (multiple-input multiple-output) concept in wireless communications [1]

that can provide high-capacity (i.e., spectral efficiency) wireless communications in rich scattering environments. It has been shown that the theoretical capacity (approximately) increases linearly as the number of antennas is increased [1, 2].

With the advent of flexible and programmable radio technology, transmitter optimization techniques used in conjunction with MIMO processing can provide even greater gains in systems with multiple users. Reconfigurable radio platforms are particularly suitable for implementation of transmitter optimization at the base station. Such optimization techniques have great potential to enhance performance on the downlink of multiuser wireless systems. From an information-theoretic model, the downlink corresponds

This is an open access article distributed under the Creative Commons Attribution License, which permits unrestricted use, distribution, and reproduction in any medium, provided the original work is properly cited.

to the case of a *broadcast channel* [3]. Recent studies that have also focussed on multiple-antenna systems with multiple users include [4, 5, 6, 7, 8, 9, 10] and the references therein.

In this paper, we study multiple-antenna transmitter optimization (i.e., spatial prefiltering) schemes that are based on linear preprocessing and transmit power optimization (keeping the average transmit power conserved). Specifically, we consider the downlink of a wireless system with multiple transmit antennas at the base station and a number of mobile terminals (i.e., users) each with a single receive antenna. We consider the maximum achievable sum data rates in the case of (1) zero-forcing spatial prefilter, (2) modified zero-forcing spatial prefilter, and (3) triangularization spatial prefilter coupled with dirty-paper coding transmission scheme [11]. We study the relationship between the above schemes as well as the impact of the number of antennas on performance.

After characterizing the fundamental performance limits, we then study the performance of the above transmitter optimization schemes with respect to delayed channel state information (CSI). The delay in CSI may be attributed to the delay in feeding back this information from the mobiles to the base station or alternately to the delays in the ability to reprogram/reconfigure the transmitter prefilter. Without explicitly characterizing the source and the nature of such delays, we show how the performance of the above transmitter optimization schemes is degraded by the CSI delay. In order to alleviate this problem, we exploit correlations in the channel by designing a linear MMSE predictor of the channel state. We then show how the application of the MMSE predictor can improve performance of transmitter optimization schemes under delayed CSI.

The paper is organized as follows. In Section 2 we describe the system model. In Section 3, we describe the various transmitter optimization schemes including their fundamental performance limits as well as the effect of delayed CSI. In Section 4, a formal channel model capturing channel correlations and a linear MMSE predictor of the channel state which is used to overcome the effect of delayed CSI are presented.

2. SYSTEM MODEL

In the following we introduce the system model. We use a MIMO model [1] that corresponds to a system presented in Figure 1. It consists of M transmit antennas and N mobile terminals (each with a single receive antenna). In other words each mobile terminal presents a MISO channel as seen from the base station.

In Figure 1, x_n is the information bearing signal intended for mobile terminal n and y_n is the received signal at the corresponding terminal (for $n = 1, \dots, N$). The received vector $\mathbf{y} = [y_1, \dots, y_N]^T$ is

$$\mathbf{y} = \mathbf{H}\mathbf{S}\mathbf{x} + \mathbf{n}, \quad \mathbf{y} \in \mathbb{C}^N, \mathbf{x} \in \mathbb{C}^N, \mathbf{n} \in \mathbb{C}^N, \quad (1)$$

$$\mathbf{S} \in \mathbb{C}^{M \times N}, \mathbf{H} \in \mathbb{C}^{N \times M},$$

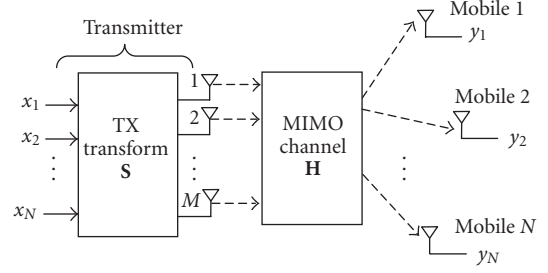


FIGURE 1: System model consisting of M transmit antennas and N mobile terminals.

where $\mathbf{x} = [x_1, \dots, x_N]^T$ is the transmitted vector ($E[\mathbf{x}\mathbf{x}^H] = P_{av}\mathbf{I}_{N \times N}$), \mathbf{n} is AWGN ($E[\mathbf{n}\mathbf{n}^H] = N_0\mathbf{I}_{N \times N}$), \mathbf{H} is the MIMO channel response matrix, and \mathbf{S} is a transformation (spatial prefiltering) performed at the transmitter. Note that the vectors \mathbf{x} and \mathbf{y} have the same dimensionality. Further, h_{nm} is the n th row and m th column element of the matrix \mathbf{H} corresponding to a channel between mobile terminal n and transmit antenna m . If not stated otherwise, we will assume that $N \leq M$.

Application of the spatial prefiltering results in the composite MIMO channel \mathbf{G} given as

$$\mathbf{G} = \mathbf{H}\mathbf{S}, \quad \mathbf{G} \in \mathbb{C}^{N \times N}, \quad (2)$$

where g_{nm} is the n th row and m th column element of the composite MIMO channel response matrix \mathbf{G} . The signal received at the n th mobile terminal is

$$y_n = \underbrace{g_{nn}x_n}_{\text{Desired signal for user } n} + \underbrace{\sum_{i=1, i \neq n}^N g_{ni}x_i}_{\text{Interference}} + n_n. \quad (3)$$

In the above representation, the interference is the signal that is intended for mobile terminals other than terminal n . As said earlier, the matrix \mathbf{S} is a spatial prefilter at the transmitter. It is determined based on optimization criteria that we address in the next section and has to satisfy the constraint

$$\text{trace}(\mathbf{S}\mathbf{S}^H) \leq N \quad (4)$$

which keeps the average transmit power conserved. We represent the matrix \mathbf{S} as

$$\mathbf{S} = \mathbf{A}\mathbf{P}, \quad \mathbf{A} \in \mathbb{C}^{M \times N}, \mathbf{P} \in \mathbb{C}^{N \times N}, \quad (5)$$

where \mathbf{A} is a linear transformation and \mathbf{P} is a diagonal matrix. \mathbf{P} is determined such that the transmit power remains conserved.

3. TRANSMITTER OPTIMIZATION SCHEMES

Considering different forms of the matrix \mathbf{A} , we study the following transmitter optimization schemes.

(1) *Zero-forcing (ZF) spatial prefiltering scheme* where \mathbf{A} is represented by

$$\mathbf{A} = \mathbf{H}^H (\mathbf{H}\mathbf{H}^H)^{-1}. \quad (6)$$

As can be seen, for $N \leq M$, the above linear transformation is zeroing the interference between the signals dedicated to different mobile terminals, that is, $\mathbf{H}\mathbf{A} = \mathbf{I}_{N \times N}$. x_n are assumed to be circularly symmetric complex random variables having Gaussian distribution $\mathcal{N}_c(0, P_{av})$. Consequently, the maximum achievable data rate (capacity) for mobile terminal n is

$$R_n^{ZF} = \log_2 \left(1 + \frac{P_{av} |p_{nn}|^2}{N_0} \right), \quad (7)$$

where p_{nn} is the n th diagonal element of the matrix \mathbf{P} defined in (5). In (6) it is assumed that $\mathbf{H}\mathbf{H}^H$ is invertible, that is, the rows of \mathbf{H} are linearly independent.

(2) *Modified zero-forcing (MZF) spatial prefiltering scheme* that assumes

$$\mathbf{A} = \mathbf{H}^H \left(\mathbf{H}\mathbf{H}^H + \frac{N_0}{P_{av}} \mathbf{I} \right)^{-1}. \quad (8)$$

In the case of the above transformation, in addition to the knowledge of the channel \mathbf{H} , the transmitter has to know the noise variance N_0 . x_n are assumed to be circularly symmetric complex random variables having Gaussian distribution $\mathcal{N}_c(0, P_{av})$. The maximum achievable data rate (capacity) for mobile terminal n now becomes

$$R_n^{MZF} = \log_2 \left(1 + \frac{P_{av} |g_{nn}|^2}{P_{av} \sum_{i=1, i \neq n}^N |g_{ni}|^2 + N_0} \right). \quad (9)$$

While the transformation in (8) appears to be similar in form to an MMSE linear receiver, the important difference is that the transformation is performed at the transmitter. Using the virtual uplink approach for transmitter beamforming (introduced in [7, 8]), we present the following proposition.

Proposition 1. *If the n th diagonal element of \mathbf{P} is selected as*

$$p_{nn} = \frac{1}{\sqrt{\mathbf{a}_n^H \mathbf{a}_n}} \quad (n = 1, \dots, N), \quad (10)$$

where \mathbf{a}_n is the n th column vector of the matrix \mathbf{A} , the constraint in (4) is satisfied with equality. Consequently, the achievable downlink rate R_n^{MZF} for mobile n is identical to its corresponding virtual uplink rate when an optimal uplink linear MMSE receiver is applied.

See Appendix A for a definition of the corresponding virtual uplink and a proof of the above proposition.

(3) *Triangularization spatial prefiltering with dirty-paper coding (DPC)* where the matrix \mathbf{A} assumes the form

$$\mathbf{A} = \mathbf{H}^H \mathbf{R}^{-1}, \quad (11)$$

where $\mathbf{H} = (\mathbf{Q}\mathbf{R})^H$ and \mathbf{Q} is unitary and \mathbf{R} is upper triangular (see [12] for details on \mathbf{QR} factorization). In general, \mathbf{R}^{-1} is a pseudoinverse of \mathbf{R} . The composite MIMO channel \mathbf{G} in (2) becomes $\mathbf{G} = \mathbf{L} = \mathbf{H}\mathbf{S}$, a lower triangular matrix. It permits application of dirty-paper coding designed for single-input single-output (SISO) systems. We refer the reader to [4, 5, 6, 13, 14, 15, 16] for further details on the DPC schemes.

By applying the transformation in (11), the signal intended for terminal 1 is received without interference. The signal at terminal 2 suffers from the interference arising from the signal dedicated to terminal 1. In general, the signal at terminal n suffers from the interference arising from the signals dedicated to terminals 1 to $n - 1$. In other words,

$$\begin{aligned} y_1 &= g_{11}x_1 + n_1, \\ y_2 &= g_{22}x_2 + g_{21}x_1 + n_2, \\ &\vdots \\ y_n &= g_{nn}x_n + \sum_{i=1}^{n-1} g_{ni}x_i + n_n, \\ &\vdots \\ y_N &= g_{NN}x_N + \sum_{i=1}^{N-1} g_{Ni}x_i + n_N. \end{aligned} \quad (12)$$

Since the interference is known at the transmitter, DPC can be applied to mitigate the interference (the details are given in Appendix B). Based on the results in [13], the achievable rate for mobile terminal n is

$$R_n^{DPC} = \log_2 \left(1 + \frac{P_{av} |g_{nn}|^2}{N_0} \right) = \log_2 \left(1 + \frac{P_{av} |r_{nn} p_{nn}|^2}{N_0} \right), \quad (13)$$

where r_{nn} is the n th diagonal element of the matrix \mathbf{R} defined in (11). Note that DPC is applied just in the case of the linear transformation in (11), with corresponding rate given by (13).

Note that $\text{trace}(\mathbf{A}\mathbf{A}^H) = N$, thereby satisfying the constraint in (4). Consequently, we can select $\mathbf{P} = \mathbf{I}_{N \times N}$ and present the following proposition.

Proposition 2. *For high SNR ($P_{av} \gg N_0$) and $\mathbf{P} = \mathbf{I}_{N \times N}$, the achievable sum rate of the triangularization with DPC scheme is equal to the rate of the equivalent (open loop) MIMO system. In other words, for $P_{av} \gg N_0$,*

$$\sum_{n=1}^N R_n^{DPC} = \log_2 \left(\det \left(\mathbf{I}_{N \times N} + \frac{P_{av}}{N_0} \mathbf{H}\mathbf{H}^H \right) \right). \quad (14)$$

Proof. Starting from the right-side term in (14) and with $\mathbf{H}\mathbf{H}^H = \mathbf{R}^H\mathbf{R}$, for $P_{av} \gg N_0$,

$$\begin{aligned}
 & \log_2 \left(\det \left(\mathbf{I}_{N \times N} + \frac{P_{av}}{N_0} \mathbf{R}^H \mathbf{R} \right) \right) \\
 & \approx \log_2 \left(\det \left(\frac{P_{av}}{N_0} \mathbf{R}^H \mathbf{R} \right) \right) \\
 & = \log_2 \left(\frac{P_{av}}{N_0} |r_{11}|^2 \cdots \frac{P_{av}}{N_0} |r_{NN}|^2 \right) \\
 & = \sum_{i=1}^N \log_2 \left(\frac{P_{av}}{N_0} |r_{ii}|^2 \right) \approx \sum_{i=1}^N \log_2 \left(1 + \frac{P_{av}}{N_0} |r_{ii}|^2 \right) \\
 & = \sum_{n=1}^N R_n^{\text{DPC}}
 \end{aligned} \tag{15}$$

which concludes the proof. \square

The ZF and MZF schemes should be viewed as transmitter beamforming techniques using conventional channel coding to approach the achievable rates [7, 8]. The triangularization with DPC scheme is necessarily coupled with a nonconventional coding, that is, the DPC scheme.

Once the matrix \mathbf{A} is selected, the elements of the diagonal matrix \mathbf{P} are determined such that the transmit power remains conserved and the sum rate is maximized. The constraint on the transmit power is

$$\text{trace}(\mathbf{A}\mathbf{P}\mathbf{P}^H\mathbf{A}^H) \leq N. \tag{16}$$

The elements of the matrix \mathbf{P} are selected such that

$$\begin{aligned}
 \text{diag}(\mathbf{P}) &= [p_{11}, \dots, p_{NN}]^T \\
 &= \arg \max_{\text{trace}(\mathbf{A}\mathbf{P}\mathbf{P}^H\mathbf{A}^H) \leq N} \sum_{i=1}^N R_n.
 \end{aligned} \tag{17}$$

3.1. Fundamental limits

To evaluate the performance of the above schemes, we consider the following baseline solutions.

(1) No prefiltering solution where each mobile terminal is served by one transmit antenna dedicated to that mobile. This is equivalent to $\mathbf{S} = \mathbf{I}$. A transmit antenna is assigned to a particular terminal corresponding to the best channel (maximum channel magnitude) among all available transmit antennas and that terminal.

(2) Equal resource TDMA and coherent beamforming (denoted as TDMA-CBF) is a solution where signals for different terminals are sent in different (isolated) time slots. In this case, there is no interference, and each terminal is using $1/N$ of the overall resources. When serving a particular mobile, ideal coherent beamforming is applied using all M transmit antennas.

(3) Closed-loop MIMO (using the water-pouring optimization on eigenmodes) is a solution that is used as an upper bound on the achievable sum rates. In the following, it is denoted as CL-MIMO. This solution would require that multiple terminals act as a joint multiple-antenna receiver.

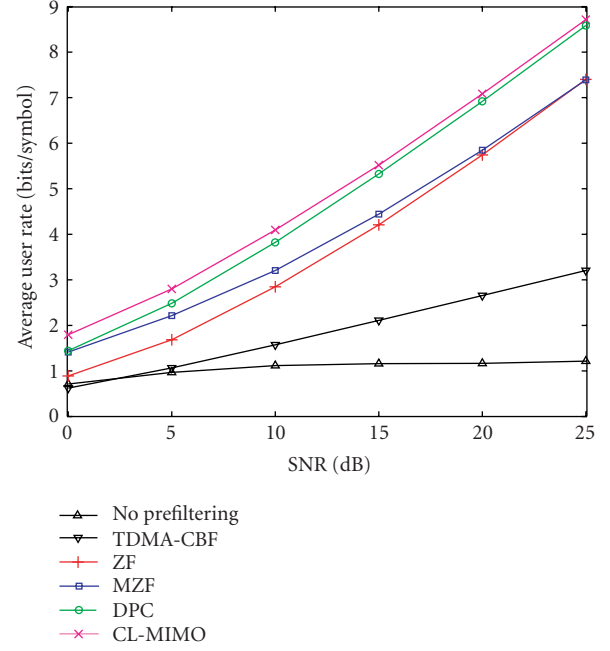


FIGURE 2: Average rate per user versus SNR ($M = 3$, $N = 3$, Rayleigh channel).

This solution is not practical because the terminals are normally individual entities in the network and they do not cooperate when receiving signals on the downlink.

In Figure 2, we present average rates per user versus $\text{SNR} = 10 \log(P_{av}/N_0)$ for a system consisting of $M = 3$ transmit antennas and $N = 3$ terminals. The channel is Rayleigh, that is, the elements of the matrix \mathbf{H} are complex independent and identically distributed Gaussian random variables with distribution $\mathcal{N}_c(0, 1)$. From the figure we observe the following. The triangularization with DPC scheme is approaching the closed-loop MIMO rates for higher SNR. The MZF solution is performing very well for lower SNRs (approaching CL-MIMO and DPC rates), while for higher SNRs, the rates for the ZF scheme are converging to the MZF rates. The TDMA-CBF rates are increasing with SNR, but still significantly lower than the rates of the proposed optimization schemes. The solution where no prefiltering is applied clearly exhibits properties of an interference limited system (i.e., after a certain SNR, the rates are not increasing). Corresponding cumulative distribution functions (cdf) of the sum rates normalized by the number of users are given in Figure 3 for SNR = 10 dB (see more on the “capacity-versus-outage” approach in [17]).

In Figure 4, we present the behavior of the average rates per user versus number of transmit antennas. The average rates are observed for SNR = 10 dB, $N = 3$, and variable number of transmit antennas ($M = 3, 6, 12, 24$). The rates increase with the number of transmit antennas and the difference between the rates for different schemes becomes smaller. As the number of transmit antennas increases, while keeping the number of users N fixed, the spatial channels (i.e., rows of the matrix \mathbf{H}) are getting less cross-correlated (approaching

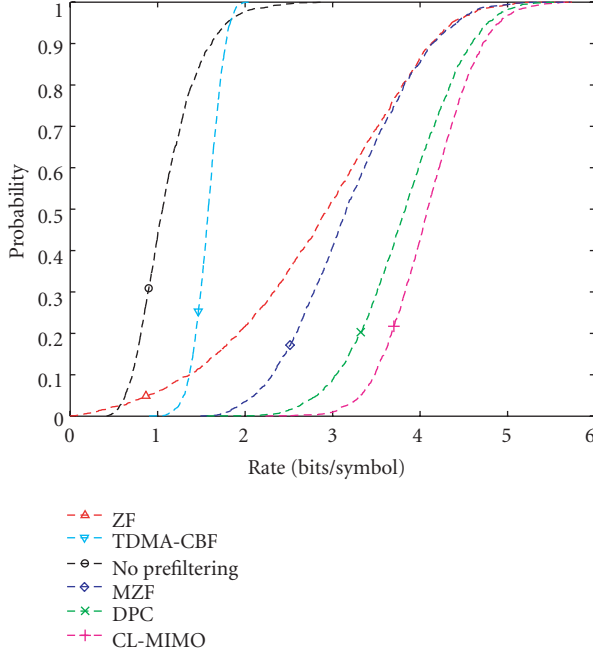


FIGURE 3: CDF of rates, SNR = 10 dB, per user ($M = 3$, $N = 3$, Rayleigh channel).

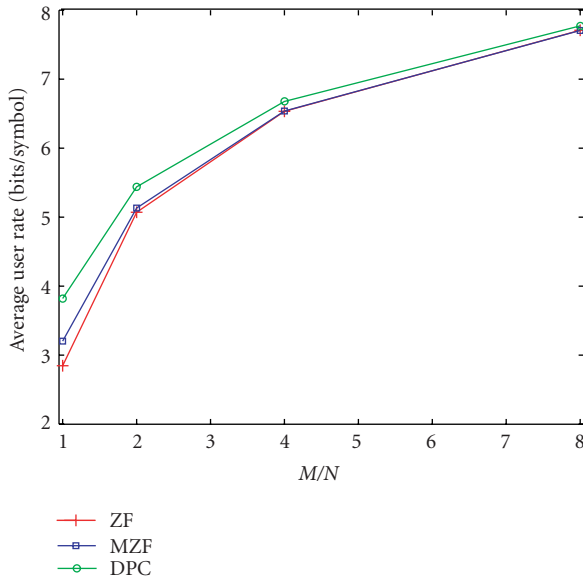


FIGURE 4: Average rate per user versus M/N (SNR = 10 dB, $N = 3$, variable number of transmit antennas $M = 3, 6, 12, 24$, Rayleigh channel).

orthogonality for $M \rightarrow \infty$). It can be shown that for orthogonal channels, all three schemes perform identically.

We now illustrate a case when the number of available terminals N_t (i.e., users) is equal to or greater than the number of transmit antennas M . Out of N_t terminals, the transmitter will select $N = M$ terminals and perform the above transmitter optimization schemes for the selected set. There are $N_t! / ((N_t - M)!M!)$ possible sets. Between the transmit

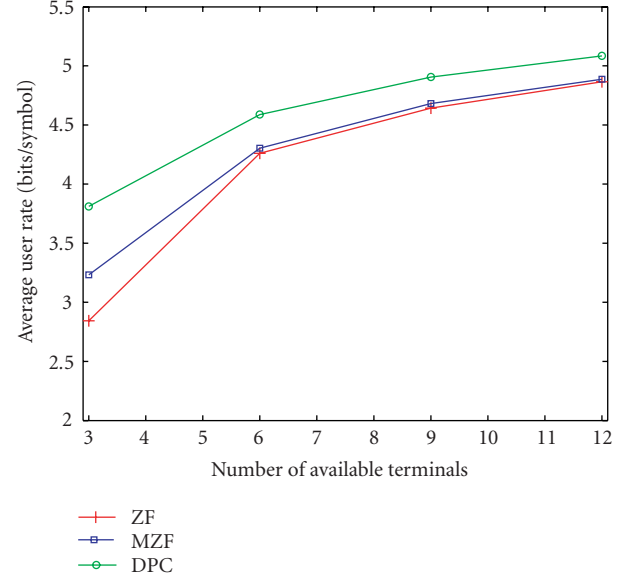


FIGURE 5: Average rate per user versus number of available terminals (SNR = 10 dB, $M = 3$, Rayleigh channel).

antennas and each terminal, there is $(1 \times M)$ -dimensional spatial channel. For each set of the terminals there is a matrix channel $\mathbf{H}_j \in \mathbb{C}^{M \times M}$ where each row corresponds to a different spatial channel of the corresponding terminal in the set. The selected terminals are the ones corresponding to the set

$$J = \arg \min_j \left\| \mathbf{H}_j^H (\mathbf{H}_j \mathbf{H}_j^H)^{-1} \right\|, \quad (18)$$

where $\|\cdot\|$ is the Frobenius norm. The above criterion will favor the terminals whose spatial channels have low cross-correlation. In Figure 5, we present the average rates per user (the average sum rates divided by $N = M$) versus number of available terminals. The increase in the rates with the number of available terminals is a result of multiuser diversity (i.e., having more terminals allows the transmitter to select more favorable channels).

3.2. Effect of CSI delay

As a motivation for the analysis presented in the following sections, we now present the effects of imperfect channel state knowledge. In practical communication systems the channel state \mathbf{H} has to be estimated at the receivers, and then fed to the transmitter. Specifically, mobile terminal n feeds back the estimate of the n th row of the matrix \mathbf{H} , for $n = 1, \dots, N$. In the case of a time-varying channel, this practical procedure results in noisy and delayed (temporally mismatched) estimates being available to the transmitter to perform the optimization. As said earlier, the MIMO channel is time varying. Let \mathbf{H}_{i-1} and \mathbf{H}_i correspond to consecutive block-faded channel responses. The temporal characteristic of the channel is described using the correlation

$$k = \frac{\mathbb{E}[h_{(i-1)nm} h_{inm}^*]}{\Gamma}, \quad (19)$$

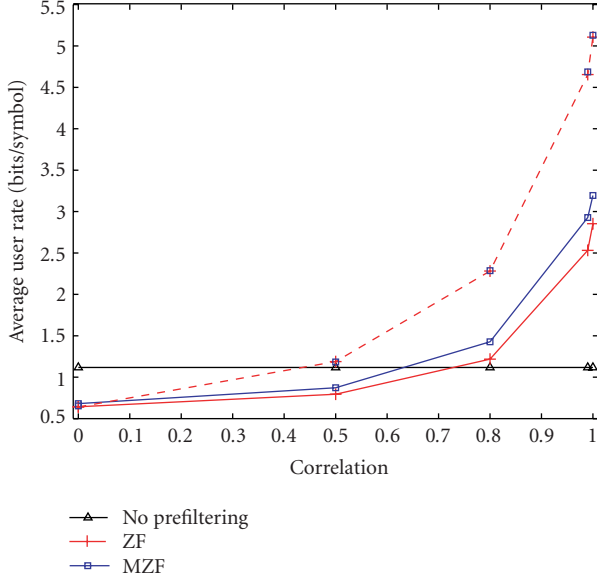


FIGURE 6: Average rate per user versus temporal channel correlation k (SNR = 10 dB, $M = 3$ (solid lines), $M = 6$ (dashed lines), $N = 3$, Rayleigh channel).

where $\Gamma = E[h_{inm}h_{inm}^*]$, and h_{inm} is a stationary random process (for $m = 1, \dots, M$ and $n = 1, \dots, N$, denoting transmit and receive-antenna indices, respectively). Low values of the correlation k correspond to higher mismatch between \mathbf{H}_{i-1} and \mathbf{H}_i . Note that the above channel is modeled as a first-order discrete Markov process. In the case of the Jakes model, $k = J_0(2\pi f_d \tau)$, where f_d is the maximum Doppler frequency and τ is the time difference between $h_{(i-1)nm}$ and h_{inm} . In addition, the above simplified model assumes that there is no spatial correlation.

We assume that the mobile terminals feed back \mathbf{H}_{i-1} which is used at the base station to perform the transmitter optimization for the i th block. In other words, the downlink transmitter is ignoring the fact that $\mathbf{H}_i \neq \mathbf{H}_{i-1}$. In Figure 6, we present the average rate per user versus the temporal channel correlation k in (19). From these results we note the very high sensitivity of the schemes to the channel mismatch. In this particular case, the performance of the ZF and MZF schemes becomes worse than when there is no prefiltering. See also [18] for a related study of channel mismatch and achievable data rates for single-user MIMO systems. Note that the above example and the model in (19) is a simplification that we only use to illustrate the schemes' sensitivity to imperfect knowledge of the channel state. In the following section, we introduce a detailed channel model incorporating correlations in the channel state information.

4. CHANNEL STATE PREDICTION FOR PERFORMANCE ENHANCEMENT

In the following, we first address the temporal aspects of the channel \mathbf{H} . For each mobile terminal, there is a $(1 \times M)$ -dimensional channel between its receive antenna and M

transmit antennas at the base station. The MISO channel $\mathbf{h}_n = [h_{n1} \dots h_{nM}]$ for mobile terminal n ($n = 1, \dots, N$) corresponds to the n th row of the channel matrix \mathbf{H} , and we assume that it is independent of other channels (i.e., rows of the channel matrix). The temporal evolution of the MISO channel \mathbf{h}_n may be represented as [19, 20]

$$\mathbf{h}_n(t) = [1 \dots 1] \mathbf{D}_n \mathbf{N}_n, \quad \mathbf{D}_n \in \mathbb{C}^{N_f \times N_f}, \quad \mathbf{N}_n \in \mathbb{C}^{N_f \times M}, \quad (20)$$

where \mathbf{N}_n is an $(N_f \times M)$ -dimensional matrix with elements corresponding to complex i.i.d. random variables with distribution $\mathcal{N}_{\mathbb{C}}(0, 1/N_f)$. \mathbf{D}_n is an $N_f \times N_f$ diagonal Doppler shift matrix with diagonal elements

$$d_{ii} = e^{j\omega_i t} \quad (21)$$

representing the Doppler shifts that affect N_f plane waves and

$$\omega_i = \frac{2\pi}{\lambda} v_n \cos(\gamma_i), \quad \text{for } i = 1, \dots, N_f, \quad (22)$$

where v_n is the velocity of mobile terminal n and the angle of arrival of the i th plane wave at the terminal is γ_i (generated as $\mathcal{U}[0, 2\pi]$).

It can be shown that the model in (20) strictly conforms to the Jakes model for $N_f \rightarrow \infty$. This model assumes that at the mobile terminal the plane waves are coming from all directions with equal probability. Further, note that each diagonal element of \mathbf{D}_n corresponds to one Doppler shift. \mathbf{D}_n and \mathbf{N}_n are independently generated. With minor modifications, the above model can be modified to capture the spatial correlations as well (see [21]).

We assume that the transmitter has a set of previous channel responses (for mobile terminal n) $\mathbf{h}_n(t)$ where $t = kT_{\text{ch}}$ and $k = 0, -1, \dots, -(L-1)$. The time interval T_{ch} may correspond to a period when a new CSI is sent from the mobile terminal to the base station. Knowing that the wireless channel has correlations, based on previous channel responses the transmitter may perform a prediction of the channel response $\mathbf{h}_n(\tau)$ at the time moment τ . In this paper we assume that the prediction is linear and that it minimizes the mean square error between true and predicted channel state. The MMSE predictor \mathbf{W}_n is

$$\mathbf{W}_n = \min_{\mathbf{T}} \arg E \left| \mathbf{T}^H \mathbf{h}_{un} - \mathbf{h}_n(\tau)^H \right|^2, \quad (23)$$

where \mathbf{h}_{un} is a vector defined as

$$\mathbf{h}_{un} = [\mathbf{h}_n(0) \mathbf{h}_n(-T_{\text{ch}}) \dots \mathbf{h}_n(-(L-1)T_{\text{ch}})]^T. \quad (24)$$

In other words, the vector is constructed by stacking up the previous channel responses available to the transmitter. We define the following matrices:

$$\begin{aligned} \mathbf{U}_n &= E[\mathbf{h}_{un} \mathbf{h}_{un}^H], \\ \mathbf{V}_n &= E[\mathbf{h}_{un} \mathbf{h}_n(\tau)^H]. \end{aligned} \quad (25)$$

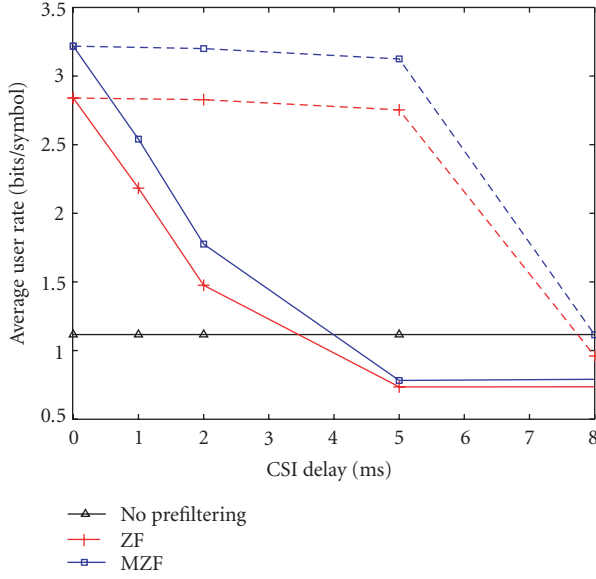


FIGURE 7: Average rate per user versus CSI delay, with MMSE prediction (dashed lines) and without MMSE prediction (solid lines) (SNR = 10 dB, $M = 3$, $N = 3$, channel based on model in (20), $f_c = 2$ GHz, $v = 30$ kmph).

It can be shown that the linear MMSE predictor \mathbf{W}_n is [22]

$$\mathbf{W}_n = \mathbf{U}_n^{-1} \mathbf{V}_n. \quad (26)$$

The above predictor exploits the correlations of the MISO channel. Note that different linear predictors are needed for different mobile terminals.

A practical implementation of the above prediction can use sample estimates of \mathbf{U}_n and \mathbf{V}_n as

$$\begin{aligned} \hat{\mathbf{U}}_n &= \frac{1}{N_w} \sum_{i=-N_w}^{-1} \mathbf{h}_{un}(iT_{\text{ch}}) \mathbf{h}_{un}(iT_{\text{ch}})^H, \\ \hat{\mathbf{V}}_n &= \frac{1}{N_w} \sum_{i=-N_w}^{-1} \mathbf{h}_{un}(iT_{\text{ch}}) \mathbf{h}_n(\tau + iT_{\text{ch}}). \end{aligned} \quad (27)$$

Underlying assumption in using the above estimates is that the channel is stationary over the integration window $N_w T_{\text{ch}}$. Further, if the update of the CSI is performed at discrete time moments kT_{ch} ($k = 0, -1, \dots$), the update period T_{ch} should be such that

$$T_{\text{ch}} < \frac{1}{2f_{\text{doppler}}}. \quad (28)$$

In Figure 7, we present the average rates per user versus the delay τ of the CSI. The system consists of $M = 3$ transmit antennas and $N = 3$ terminals. The channel is modeled based on (20) (assuming that the carrier frequency is 2 GHz and the velocity of each mobile terminal is 30 kmph and setting the number of plane waves $N_f = 100$). Because the ideal channel state $\mathbf{H}(t + \tau)$ is not available at the transmitter, we assume that $\mathbf{H}(t)$ is used instead to perform the transmitter

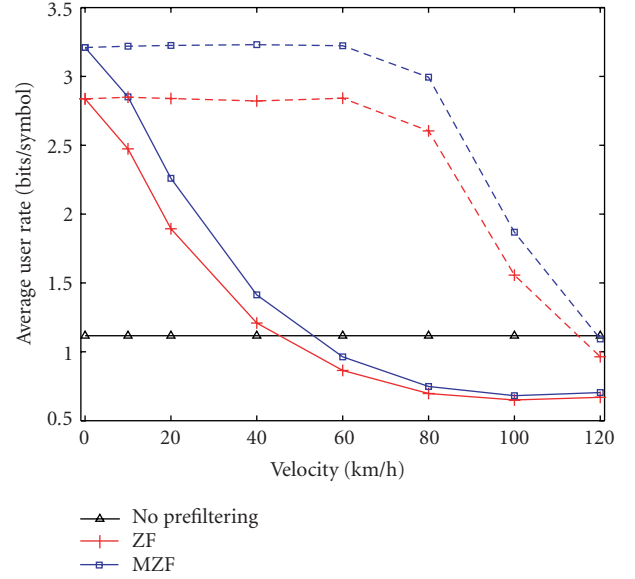


FIGURE 8: Average rate per user versus terminal velocity, with MMSE prediction (dashed lines) and without MMSE prediction (solid lines) (SNR = 10 dB, $M = 3$, $N = 3$, channel based on model in (20), $f_c = 2$ GHz, $\tau = 2$ milliseconds).

optimization at the moment $t + \tau$. Figure 7 presents average rates for the ZF and MZF schemes, for SNR = 10 dB. Results depicted by the solid lines correspond to the application of the delayed CSI $\mathbf{H}(t)$ instead of the true channel state $\mathbf{H}(t + \tau)$. The dashed lines depict results when the MMSE predicted channel state $\mathbf{H}_{\text{MMSE}}(t + \tau)$ is used instead of the true channel state $\mathbf{H}(t + \tau)$. Without any particular effort to optimally select the implementation parameters, in this particular example, we use $L = 10$ previous channel responses to construct the vectors in (24). Further, the length of the integration window in (27) is selected to be $N_w = 100$. The results clearly point to improvements in the performance of the schemes when the MMSE channel state prediction is used. The results suggest that the temporal correlations in the channel alone are significant enough to support the application of the MMSE prediction. The presence of spatial correlations in the channel model will further improve the benefits of such channel state prediction schemes used in conjunction with transmitter optimization.

For the above assumptions, in Figure 8 we present the average rates per user versus the terminal velocity with the CSI delay $\tau = 2$ milliseconds. From the results, we can see that the prediction scheme significantly extends the gains of the transmitter optimization even for higher terminal velocities.

5. CONCLUSION

The advances in programmable and reconfigurable radios have rendered feasible transmitter optimization schemes that can greatly improve the performance of multiple-antenna multiuser systems. In this paper, we presented a study on multiple-antenna transmitter optimization schemes for multiuser systems that are based on linear transformations and

transmit power optimization. We considered the maximum achievable sum data rates in the case of the zero-forcing, the modified zero-forcing, and the triangularization spatial prefiltering coupled with the dirty-paper coding transmission scheme. We showed that the triangularization with DPC approaches the closed-loop MIMO rates (upper bound) for higher SNR. Further, the MZF solution performed very well for lower SNRs (approaching closed-loop MIMO and DPC rates), while for higher SNRs, the rates for the ZF scheme converged to that of the MZF rates. A key impediment to the successful deployment of transmitter optimization schemes is the delay in the channel state information (CSI) that is used to accomplish this. We characterized the degradation in the performance of transmitter optimization schemes with respect to the delayed CSI. A linear MMSE predictor of the channel state was introduced which then improved the performance in all cases. The results have suggested that the temporal correlations in the channel alone are significant enough to support the application of the MMSE prediction. In the presence of additional spatial correlations, the usefulness of such prediction schemes will be even greater.

APPENDICES

A. DEFINITION OF THE VIRTUAL LINK AND PROOF OF PROPOSITION 1

We now describe the corresponding virtual uplink for the system in Figure 1. Let \bar{x}_n be the uplink information-bearing signal transmitted from mobile terminal n ($n = 1, \dots, N$) and let \bar{y}_m be the received signal at the m th base station antenna ($m = 1, \dots, M$). \bar{x}_n are assumed to be circularly symmetric complex random variables having Gaussian distribution $\mathcal{N}(0, P_{av})$. Further, the received vector $\bar{\mathbf{y}} = [\bar{y}_1, \dots, \bar{y}_M]^T$ is

$$\bar{\mathbf{y}} = \bar{\mathbf{H}}\bar{\mathbf{x}} + \bar{\mathbf{n}} = \mathbf{H}^H\bar{\mathbf{x}} + \bar{\mathbf{n}}, \quad \bar{\mathbf{y}} \in \mathcal{C}^M, \bar{\mathbf{x}} \in \mathcal{C}^N, \quad (\text{A.1})$$

$$\bar{\mathbf{n}} \in \mathcal{C}^M, \bar{\mathbf{H}} \in \mathcal{C}^{M \times N},$$

where $\bar{\mathbf{x}} = [\bar{x}_1, \dots, \bar{x}_N]^T$ is the transmitted vector ($E[\bar{\mathbf{x}}\bar{\mathbf{x}}^H] = P_{av}\mathbf{I}_{N \times N}$), $\bar{\mathbf{n}}$ is AWGN ($E[\bar{\mathbf{n}}\bar{\mathbf{n}}^H] = N_0\mathbf{I}_{M \times M}$), and $\bar{\mathbf{H}} = \mathbf{H}^H$ is the uplink MIMO channel response matrix.

It is well known that the MMSE receiver is the optimal linear receiver for the uplink (*multiple-access channel*) [23, 24]. It maximizes the received SINR (and rate) for each user. The decision statistic is obtained after the receiver MMSE filtering as

$$\bar{\mathbf{x}}^{\text{dec}} = \mathbf{W}^H\bar{\mathbf{y}}, \quad (\text{A.2})$$

where the MMSE receiver is

$$\mathbf{W} = \left(\left(\mathbf{H}\mathbf{H}^H + \frac{N_0}{P_{av}}\mathbf{I} \right)^{-1} \mathbf{H} \right)^H \quad (\text{A.3})$$

$$= \mathbf{H}^H \left(\mathbf{H}\mathbf{H}^H + \frac{N_0}{P_{av}}\mathbf{I} \right)^{-1}.$$

Proof of Proposition 1. Note that $\mathbf{W} = \mathbf{A}$ in (8), for the MZF transmitter spatial prefiltering. We normalize the column vectors of the matrix \mathbf{W} in (A.3) as

$$\mathbf{W}_{\text{nor}} = \mathbf{W}\mathbf{P}, \quad (\text{A.4})$$

where \mathbf{P} is defined in (10). In other words, the n th diagonal element of \mathbf{P} is selected as

$$p_{nn} = \frac{1}{\sqrt{\mathbf{w}_n^H \mathbf{w}_n}} \quad (n = 1, \dots, N), \quad (\text{A.5})$$

where \mathbf{w}_n is the n th column vector of the matrix \mathbf{W} (where $\mathbf{w}_n = \mathbf{a}_n$, which is the column vector of \mathbf{A} for $n = 1, \dots, N$). It is well known that any normalization of the columns of the MMSE receiver in (A.3) does not change the SINRs. In other words, the SINR for the n th uplink user ($n = 1, \dots, N$) is

$$\text{SINR}_n^{\text{UL}} = \frac{P_{av} |\mathbf{w}_n^H \bar{\mathbf{h}}_n|^2}{P_{av} \sum_{i=1, i \neq n}^N |\mathbf{w}_n^H \bar{\mathbf{h}}_i|^2 + N_0 \mathbf{w}_n^H \mathbf{w}_n} \quad (\text{A.6})$$

$$= \frac{P_{av} |\mathbf{w}_n^H \bar{\mathbf{h}}_n|^2 / (\mathbf{w}_n^H \mathbf{w}_n)}{P_{av} \sum_{i=1, i \neq n}^N |\mathbf{w}_n^H \bar{\mathbf{h}}_i|^2 / (\mathbf{w}_n^H \mathbf{w}_n) + N_0},$$

where $\bar{\mathbf{h}}_n$ is the n th column vector of the matrix $\bar{\mathbf{H}}$. Note that $\bar{\mathbf{h}}_n^H = \mathbf{h}_n$ which is the n th row vector of the downlink MIMO channel \mathbf{H} . The corresponding downlink SINR when the MZF spatial prefiltering is used (with \mathbf{P} defined in (10)) is

$$\text{SINR}_n^{\text{MZF}} = \frac{P_{av} |\mathbf{h}_n \mathbf{a}_n|^2 / (\mathbf{a}_n^H \mathbf{a}_n)}{P_{av} \sum_{i=1, i \neq n}^N |\mathbf{h}_i \mathbf{a}_i|^2 / (\mathbf{a}_i^H \mathbf{a}_i) + N_0}. \quad (\text{A.7})$$

As said earlier, $\mathbf{w}_n = \mathbf{a}_n$ and $\bar{\mathbf{h}}_n^H = \mathbf{h}_n$. Thus, $\text{SINR}_n^{\text{MZF}} = \text{SINR}_n^{\text{UL}}$ for $n = 1, \dots, N$ leading to identical rates, which concludes the proof. \square

B. SPATIAL PREFILTERING WITH DPC

One practical, but suboptimal, single-dimensional DPC solution is described in [14, 15]. Starting from that solution we introduce the DPC scheme.

The transmitted signal in (1) intended for terminal n is

$$x_n = f_{\text{mod}}(\hat{x}_n - I_n), \quad (\text{B.1})$$

where \hat{x}_n is the information-bearing signal for terminal n and $f_{\text{mod}}(\cdot)$ is a modulo operation (i.e., a uniform scalar quantizer). For a real variable x , $f_{\text{mod}}(x)$ is defined as

$$f_{\text{mod}}(x) = ((x + Z) \bmod (2Z)) - Z \quad (\text{B.2})$$

and in the case of a complex variable $a + jb$, $f_{\text{mod}}(a + jb) = f_{\text{mod}}(a) + j f_{\text{mod}}(b)$. The constant Z is selected such that $E[x_n x_n^*] = P_{av}$. Further, from (12), I_n is the normalized interference at terminal n :

$$I_n = \sum_{i=1}^{n-1} \frac{g_{ni} x_i}{g_{nn}}, \quad (\text{B.3})$$

assuming that $g_{nn} \neq 0$. Note that I_n is only known at the transmitter. At terminal n , the following operation is performed:

$$f_{\text{mod}}\left(\frac{y_n}{g_{nn}}\right) = \hat{x}_n + n_n^*, \quad (\text{B.4})$$

where n_n^* is a wrapped-around AWGN (due to the nonlinear operation $f_{\text{mod}}(\cdot)$). For high SNR and with \hat{x}_n being uniformly distributed over the single-dimensional region, the achievable rate is approximately 1.53 dB away from the rate in (13) [14, 15].

To further approach the rate in (13), based on [14], the following modifications of the suboptimal scheme in (B.1) are needed. The transmitted signal intended for terminal n is now

$$x_n = f_k(\hat{x}_n - \xi_n I_n + d_n), \quad (\text{B.5})$$

where $f_k(\cdot)$ is a modulo operation over a k -dimensional region. ξ_n is a parameter to be optimized ($0 < \xi_n \leq 1$) and d_n is a dither (uniformly distributed pseudonoise over the k -dimensional region). At terminal n , the following operation is performed:

$$f_k\left(\frac{y_n}{g_{nn}}\right) = \hat{x}_n + (1 - \xi_n)u_n + \xi_n n_n^*, \quad (\text{B.6})$$

where n_n^* is a wrapped-around AWGN (due to the nonlinear operation $f_k(\cdot)$) and u_n is uniformly distributed over the k -dimensional region. For $k \rightarrow \infty$ and \hat{x}_n being uniformly distributed over the k -dimensional region, the rate in (13) can be achieved [14]. Further details on selecting ξ_n and d_n are beyond the scope of this paper. We refer the reader to [14] and references therein.

ACKNOWLEDGMENT

This work is supported in part by the National Science Foundation under Grant no. FMF 0429724.

REFERENCES

- [1] G. J. Foschini, "Layered space-time architecture for wireless communication in a fading environment when using multiple antennas," *Bell Labs Technical Journal*, vol. 1, no. 2, pp. 41–59, 1996.
- [2] G. J. Foschini and M. J. Gans, "On limits of wireless communications in a fading environment when using multiple antennas," *Wireless Personal Communications*, vol. 6, no. 3, pp. 311–335, 1998.
- [3] T. M. Cover and J. A. Thomas, *Elements of Information Theory*, John Wiley & Sons, New York, NY, USA, 1st edition, 1991.
- [4] G. Caire and S. Shamai, "On the achievable throughput of a multiantenna Gaussian broadcast channel," *IEEE Trans. Inform. Theory*, vol. 49, no. 7, pp. 1691–1706, 2003.
- [5] D. N. C. Tse and P. Viswanath, "On the capacity region of the vector Gaussian broadcast channel," in *Proc. IEEE International Symposium on Information Theory (ISIT '03)*, pp. 342–342, Yokohama, Japan, June–July 2003.
- [6] S. Vishwanath, G. Kramer, S. Shamai, S. Jafar, and A. Goldsmith, "Capacity bounds for Gaussian vector broadcast channels," in *Proc. DIMACS Workshop on Signal Processing for Wireless Transmission*, vol. 62, pp. 107–122, Rutgers University, Piscataway, NJ, USA, October 2002.
- [7] E. Rashid-Farrohi, L. Tassiulas, and K. J. R. Liu, "Joint optimal power control and beamforming in wireless networks using antenna arrays," *IEEE Trans. Commun.*, vol. 46, no. 10, pp. 1313–1324, 1998.
- [8] E. Visotsky and U. Madhow, "Optimum beamforming using transmit antenna arrays," in *Proc. 49th IEEE Vehicular Technology Conference (VTC '99)*, vol. 1, pp. 851–856, Houston, Tex, USA, May 1999.
- [9] E. Visotsky and U. Madhow, "Space-time transmit precoding with imperfect feedback," *IEEE Trans. Inform. Theory*, vol. 47, no. 6, pp. 2632–2639, 2001.
- [10] S. Thoen, L. Van der Perre, M. Engels, and H. De Man, "Adaptive loading for OFDM/SDMA-based wireless networks," *IEEE Trans. Commun.*, vol. 50, no. 11, pp. 1798–1810, 2002.
- [11] D. Samardzija and N. Mandayam, "Multiple antenna transmitter optimization schemes for multiuser systems," in *Proc. 58th IEEE Vehicular Technology Conference (VTC '03)*, vol. 1, pp. 399–403, Orlando, Fla, USA, October 2003.
- [12] G. Strang, *Linear Algebra and Its Applications*, Harcourt Brace Jovanovich, San Diego, Calif, USA, 3rd edition, 1988.
- [13] M. H. M. Costa, "Writing on dirty paper (Corresp.)," *IEEE Trans. Inform. Theory*, vol. 29, no. 3, pp. 439–441, 1983.
- [14] G. J. Foschini and A. H. Diaz, "Dirty paper coding: perturbing off the infinite dimensional lattice limit," in *Proc. DIMACS Workshop on Signal Processing for Wireless Transmission*, vol. 62, pp. 141–160, Rutgers University, Piscataway, NJ, USA, October 2002.
- [15] U. Erez, R. Zamir, and S. Shamai, "Additive noise channels with side information at the transmitter," in *Proc. 21st IEEE Convention of Electrical and Electronic Engineers in Israel*, pp. 373–376, Tel-Aviv, Israel, April 2000.
- [16] A. S. Cohen and A. Lapidoth, "Generalized writing on dirty paper," in *Proc. IEEE International Symposium on Information Theory (ISIT '02)*, pp. 227–227, Lausanne, Switzerland, June–July 2002.
- [17] E. Biglieri, J. Proakis, and S. Shamai, "Fading channels: information-theoretic and communications aspects," *IEEE Trans. Inform. Theory*, vol. 44, no. 6, pp. 2619–2692, 1998.
- [18] D. Samardzija and N. Mandayam, "Pilot-assisted estimation of MIMO fading channel response and achievable data rates," *IEEE Trans. Signal Processing*, vol. 51, no. 11, pp. 2882–2890, 2003, Special Issue on MIMO.
- [19] H. Xu, D. Chizhik, H. Huang, and R. Valenzuela, "A wave-based wideband MIMO channel modeling technique," in *Proc. 13th IEEE International Symposium on Personal, Indoor and Mobile Radio Communications (PIMRC '02)*, vol. 4, pp. 1626–1630, Lisbon, Portugal, September 2002.
- [20] D. Chizhik, "Slowing the time-fluctuating MIMO channel by beam-forming," *IEEE Transactions on Wireless Communications*, vol. 3, no. 5, pp. 1554–1565, 2004.
- [21] D. Samardzija and N. Mandayam, "Downlink multiple antenna transmitter optimization on spatially and temporally correlated channels with delayed channel state information," in *Proc. Conference on Information Sciences and Systems (CISS '04)*, Princeton University, Princeton, NJ, USA, March 2004.
- [22] S. Haykin, *Adaptive Filter Theory*, Prentice-Hall, Englewood Cliffs, NJ, USA, 2nd edition, 1991.
- [23] U. Madhow and M. L. Honig, "MMSE interference suppression for direct-sequence spread-spectrum CDMA," *IEEE Trans. Commun.*, vol. 42, no. 12, pp. 3178–3188, 1994.
- [24] S. Verdú, *Multiuser Detection*, Cambridge University Press, Cambridge, UK, 1998.

Dragan Samardzija was born in Kikinda, Serbia and Montenegro, in 1972. He received the B.S. degree in electrical engineering and computer science in 1996 from the University of Novi Sad, Serbia and Montenegro, and the M.S. and Ph.D. degrees in electrical engineering from the Wireless Information Network Laboratory (WINLAB), Rutgers University, in 2000 and 2004, respectively. Since 2000 he has been with the Wireless Research Laboratory, Bell Labs, Lucent Technologies, where he is involved in research in the field of MIMO wireless systems. His research interests include detection, estimation, and information theory for MIMO wireless systems, interference cancellation, and multiuser detection for multiple-access systems. He has also been focusing on implementation aspects of various communication architectures and platforms.



Narayan Mandayam received the B.Tech. (with honors) degree in 1989 from the Indian Institute of Technology, Kharagpur, and the M.S. and Ph.D. degrees in 1991 and 1994 from Rice University, all in electrical engineering. Since 1994 he has been at Rutgers University where he is currently a Professor of electrical and computer engineering and also an Associate Director at the Wireless Information Network Laboratory (WINLAB). He was a Visiting Faculty Fellow in the Department of Electrical Engineering, Princeton University, in Fall 2002 and a Visiting Faculty at the Indian Institute of Science in Spring 2003. His research interests are in various aspects of wireless data transmission including system modeling and performance, signal processing, and radio resource management, with emphasis on open access techniques for spectrum sharing. Dr. Mandayam is a recipient of the Institute Silver Medal from the Indian Institute of Technology, Kharagpur, in 1989, and the US National Science Foundation CAREER Award in 1998. He has served as an Editor for the IEEE Journals Communication Letters and Transactions on Wireless Communications. He is a coauthor with C. Comaniciu and H. V. Poor of the book *Wireless Networks: Multiuser Detection in Cross-Layer Design*, Springer, NY, 2005.

Dmitry Chizhik is a member of technical staff in the Wireless Research Laboratory, Bell Labs, Lucent Technologies. He received a Ph.D. degree in electrophysics from the Polytechnic University, Brooklyn, NY, in 1991. His thesis work has been in ultrasonics and nondestructive evaluation. He joined the Naval Undersea Warfare Center, New London, Conn, where he did research on scattering from ocean floor, geoacoustic modeling, and shallow water acoustic propagation. In 1996 he joined Bell Laboratories, working on radio propagation modeling and measurements, using deterministic and statistical techniques. His recent work has been in measurement, modeling, and channel estimation of MIMO channels. The results are used both for determination of channel-imposed bounds on channel capacity, system performance, as well as for optimal antenna array design. His research interests are in acoustic and electromagnetic wave propagation, signal processing, and communications.

